

Supplementary Information

Na-doped g-C₃N₄/NiO 2D/2D laminate p-n heterojunctions nanosheets toward optimized photocatalytic performance

Jiapeng Gao^a, Zipeng Xing^{a,*}, Meijie Liu^a, Yichao Wang^a, Na Zhang^a, Zhenzi Li^b,
Peng Chen^{a*}, Wei Zhou^{a, b*}

^a Department of Environmental Science, School of Chemistry and Materials Science,
Key Laboratory of Functional Inorganic Material Chemistry, Ministry of Education of
the People's Republic of China, Heilongjiang University, Harbin 150080, P. R. China,
Tel: +86-451-8660-8616, Fax: +86-451-8660-8240,

Email: xingzipeng@hlju.edu.cn; jehugu@gmail.com; zwchem@hotmail.com

^b Shandong Provincial Key Laboratory of Molecular Engineering, School of
Chemistry and Chemical Engineering, Qilu University of Technology (Shandong
Academy of Sciences), Jinan 250353, P. R. China

Experimental section

Materials

Urea and sodium chloride (NaCl) were purchased from Tianjin Fengchuan Chemical Reagent Co, Ltd. Nickel nitrate ($\text{Ni}(\text{NO}_3)_2 \cdot 6\text{H}_2\text{O}$) are purchased from Tianjin Guangfu Technology Development Co, Ltd. Deionized water (DI) was used during the experiment. All chemicals were analytically pure and did not require further purification.

Characterizations

The powder X-ray diffraction (XRD) patterns were acquired on a Bruker D8 Advance diffractometer by using Cu $K\alpha$ radiation ($\lambda = 1.5406 \text{ \AA}$). Scanning electron microscopy (SEM) images were obtained with a Philips XL-30-ESEM-FEG instrument operating at 20 kV. Transmission electron microscope (TEM) JEOL JEM-2010 at an accelerating voltage of 200 kV was also used to record the electron micrographs of the samples. X-ray photoelectron spectroscopy (XPS) was measured on a PHI-5700 ESCA instrument with Al- $K\alpha$ X-ray source. UV-vis diffuse reflection spectra (DRS) were recorded on a UV-vis spectrophotometer (UV-2550, Shimadzu) with an integrating sphere attachment, and BaSO_4 was used as the reference material. Fourier transform infrared spectra (FT-IR) were detected with a PerkinElmer spectrum one system. The N_2 adsorption-desorption isotherms at 77 K were collected on an AUTOSORB-1 (Quantachrome Instruments) nitrogen adsorption apparatus. Surface area was estimated by BET method and pore-size distribution was measured from the adsorption branch of the isotherm using the Barrett-Joyner-Halenda (BJH) method.

The steady-state photoluminescence (PL) spectra were measured with a PE LS 55 spectrofluoro-photometer at excitation wavelength of 325 nm. Transient-state photoluminescence (TS-PL) spectra were recorded on a single photon counting spectrometer from (Edinburgh Instrument, FLS 920). Scanning Kelvin probe (SKP) measurements (SKP5050 system, Scotland) were performed at normal laboratory conditions. LC-MS (Shimadzu, Japan) was used to determinate the intermediate products produced during the photodegradation process. The mobile phase was methanol and deionized water in the ratio of 70:30 (v/v), and the flow rate was 1 mL/min. The injection volume was 1 μ L.

Photocatalytic degradation of CIP

The photocatalytic degradation of CIP and other fluoroquinolones were carried out in a XPA-7 rotary photochemical reactor. The simulated sunlight source was provided by a 350 W xenon lamp with a 290 nm cut-off filter. For each experiment, 50 mL of a 4 mg/L FQs aqueous solution that contained 1.0 g/L catalysts were introduced into a quartz tube. The pH of the reaction solution was adjusted by adding a 0.1% NaOH or H₂SO₄ solution. Prior to irradiation, the reaction solution was magnetically stirred in the dark for 30 min in order to obtain an adsorption-desorption equilibrium of FQs on the photocatalyst. During irradiation, aliquots of samples (1 mL) were withdrawn at predetermined time intervals and filtered through 0.22 μ m Millipore filters to remove the photocatalyst. The residual CIP in the solution were analyzed through high performance liquid chromatography (HPLC).

Photocatalytic hydrogen evolution

The photocatalytic hydrogen evolution was tested in an online photocatalytic hydrogen evolution system (Au Light, Beijing, CEL-SPH2N) at room temperature. In a typical process, 50 mg of photocatalysts were suspended in 100 mL aqueous closed gas circulation reaction cell which include 80 mL deionized water and 20 mL of methanol used as the sacrificial reagent. Afterward, the suspension was purged with N₂ for several times to remove O₂ and CO₂. After that, the suspension solution was irradiated by a 300 W Xeon-lamp equipped with an AM 1.5 G filter (Oriel, USA), and use an on-line gas chromatography (SP7800, TCD, molecular sieve 5 Å, N₂ carrier, Beijing Keruida, Ltd) to analyze the hydrogen periodically with the interval of every 1 h.

Photoelectrochemical measurements

Photoelectrochemical measurements of photocatalysts were detected in a three-electrode system with the CHI760E electrochemical workstation. The electrolyte selected KOH solution (1 M), the reference electrode selected Ag/AgCl and the opposite electrode selected Pt. Then, 0.1 g of photocatalysts were mixed with 3 mL of ethanol at stirring for 10 min, and sprayed on the FTO-glass of 1×2 cm² further heating and drying. The photocurrent test was extra monitored under AM 1.5G light exposure.

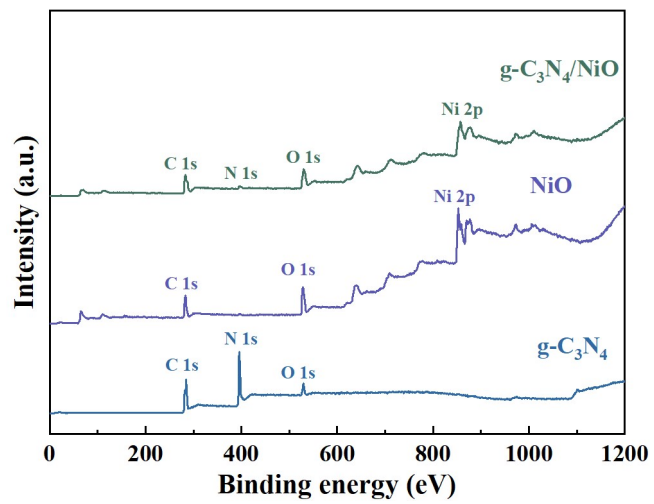


Fig. S1. The XPS survey scans of g-C₃N₄, NiO, g-C₃N₄/NiO.

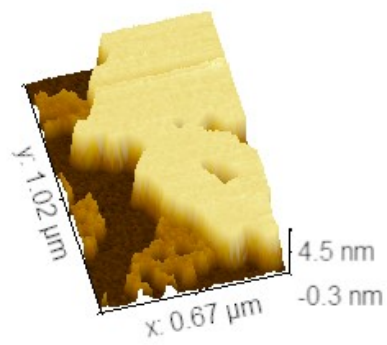


Fig. S2. The 3D AMF structure of the measured ultrathin g-C₃N₄.

Curve: Method:

Points	X [nm]	Y [nm]	Length [nm]	Height [nm]	Angle [deg]
	0.0	-0.082			
	0.0	1.306	0.0	1.388	90.00

Fig. S3. Thickness of ultra-thin g-C₃N₄.

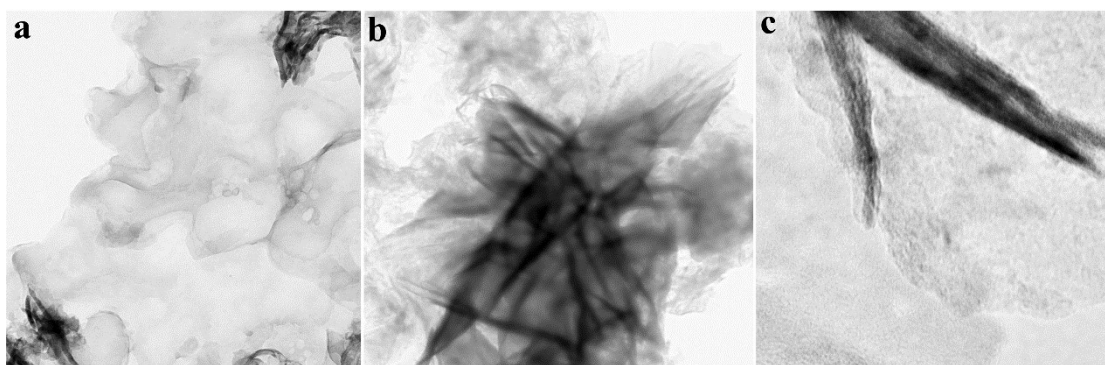


Fig. S4. TEM images of g-C₃N₄ (a) NiO (b), and Na-g-C₃N₄/NiO (c).

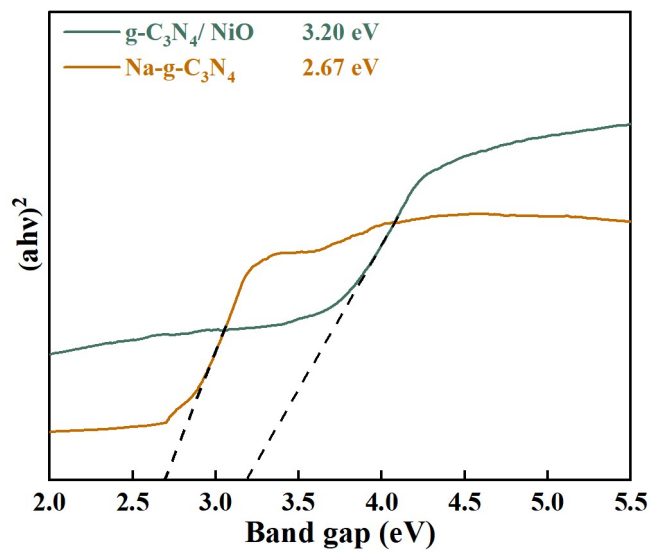


Fig. S5. The band gaps of $Na-g-C_3N_4$, and $g-C_3N_4/NiO$.

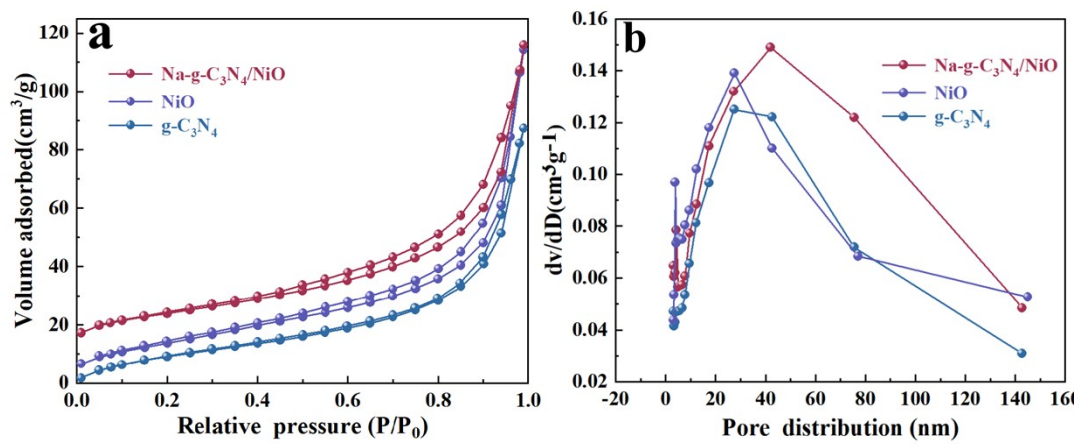


Fig. S6. The N₂ adsorption-desorption isotherms of g-C₃N₄, NiO and Na-g-C₃N₄/NiO (a) and the corresponding pore size distributions (b), respectively.

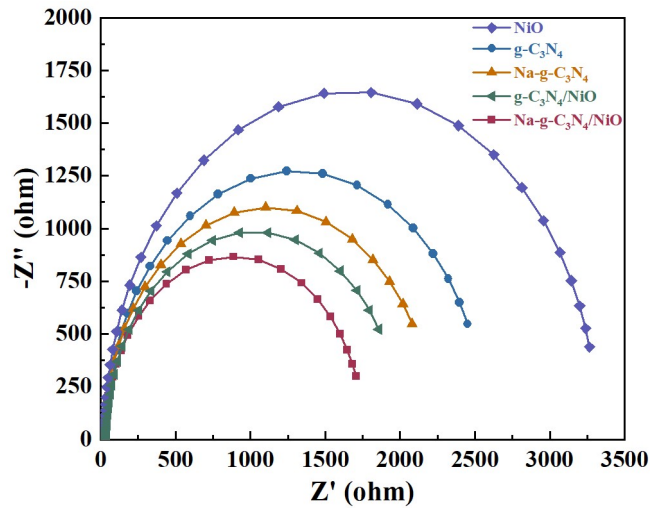


Fig. S7. Electrochemical impedance spectra of $g-C_3N_4$, $Na-g-C_3N_4$, NiO, $g-C_3N_4/NiO$ and $Na-g-C_3N_4/NiO$, respectively.

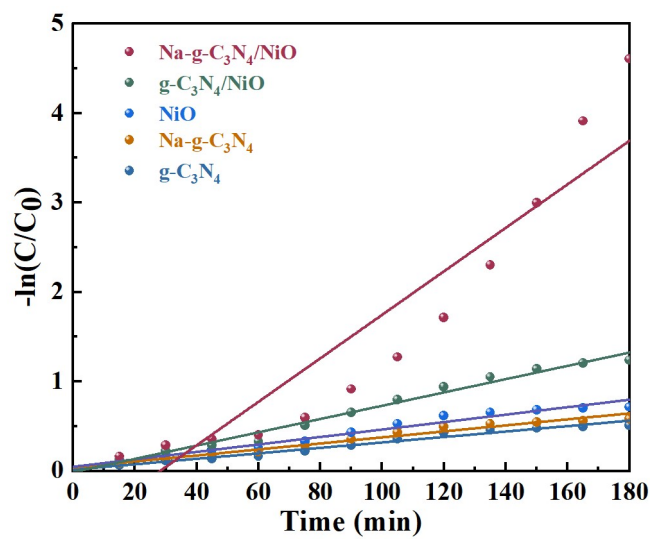


Fig. S8. The first order kinetic curves of CIP degradation for different photocatalysts.

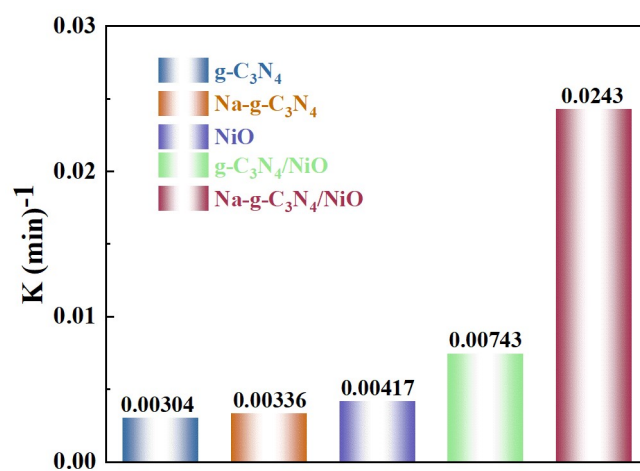


Fig. S9. The first-order reaction rate constants for photocatalytic reduction and degradation of CIP for different photocatalysts.

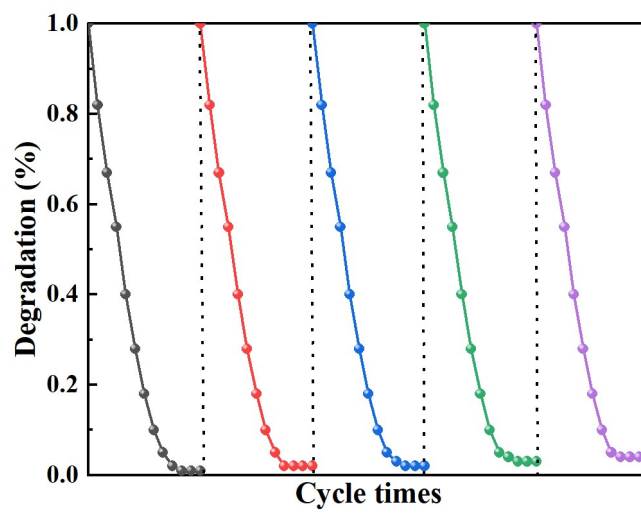


Fig. S10. Degradation cycle experiments of CIP degradation for Na-g-C₃N₄/NiO.

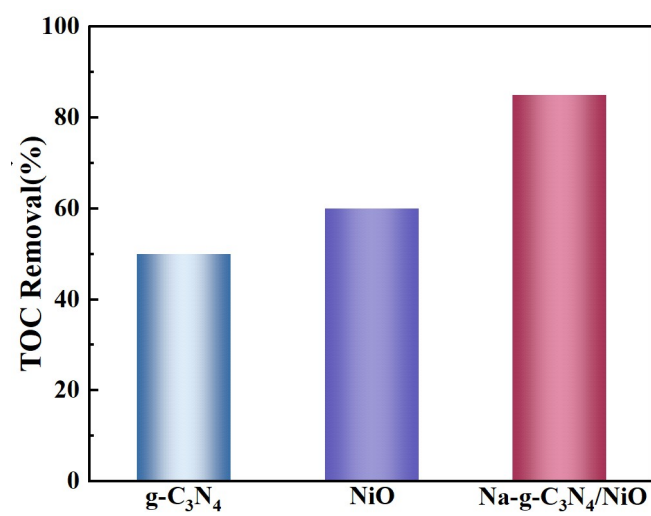


Fig. S11. The TOC removal rates of different samples for photocatalytic degrading CIP.

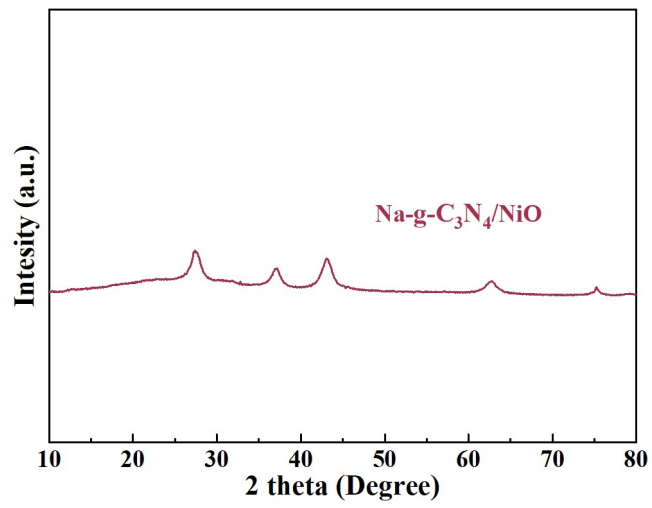


Fig. S12. XRD pattern of Na-g-C₃N₄/NiO after photocatalytic degradation.

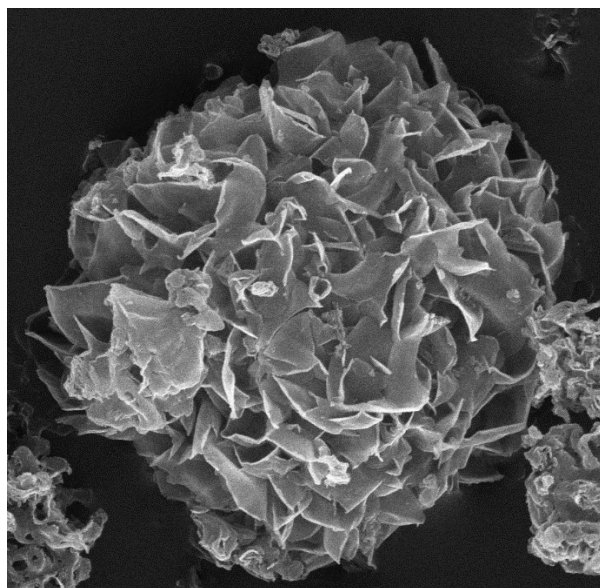


Fig. S13. SEM image of Na-g-C₃N₄/NiO after photocatalytic degradation.

Table S1. Comparison of photocatalytic H₂ evolution rates between Na-g-C₃N₄/NiO and other different photocatalysts under visible light irradiation.

Photocatalysts	Light source	H ₂ evolution rate	Ref.
g-C ₃ N ₄ (P)	300 W Xe lamp ($\lambda > 420$ nm)	916.2 $\mu\text{mol h}^{-1} \text{g}^{-1}$	[1]
N-defects g-C ₃ N ₄	300 W Xe lamp ($\lambda > 420$ nm)	1160 $\mu\text{mol h}^{-1} \text{g}^{-1}$	[2]
P-Na codoped g-C ₃ N ₄	300 W Xe lamp ($\lambda > 400$ nm)	2032 $\mu\text{mol h}^{-1} \text{g}^{-1}$	[3]
Na-g-C ₃ N ₄	350 W Xe lamp ($\lambda > 400$ nm)	18.7 $\mu\text{mol h}^{-1}$	[4]
NiO/Ni ₂ P/g-C ₃ N ₄	300 W Xe lamp ($\lambda > 420$ nm)	5.04 $\mu\text{mol h}^{-1}$	[5]
NiO QDs-g-C ₃ N ₄	300 W Xe lamp ($\lambda > 400$ nm)	260.2 $\mu\text{mol h}^{-1} \text{g}^{-1}$	[6]
Na-g-C₃N₄/NiO	300 W Xe lamp ($\lambda > 420$ nm)	2299.32 $\mu\text{mol h}^{-1} \text{g}^{-1}$	This work

References

- [1] B. Wang, H. Cai, D. Zhao, M. Song, P. Guo, S. Shen, D. Li, S. Yang, Enhanced photocatalytic hydrogen evolution by partially replaced corner-site C atom with P in g-C₃N₄, *Appl. Catal. B*, 244 (2019) 486-493.
- [2] J. Huang, Y. Cao, H. Wang, H. Yu, F. Peng, H. Zou, Z. Liu, Revealing active-site structure of porous nitrogen-defected carbon nitride for highly effective photocatalytic hydrogen evolution, *Chem. Eng. J.*, 373 (2019) 687-699.
- [3] C. Wang, W. Wang, H. Fan, N. Zhao, J. Ma, M. Zhang, A.K. Yadav, A Codoped Polymeric Photocatalyst with Prolonged Carrier Lifetime and Extended Spectral Response up to 600 nm for Enhanced Hydrogen Evolution, *ACS Appl. Mater. Interfaces*, 12 (2020) 5234-5243.
- [4] J. Jiang, S. Cao, C. Hu, C. Chen, A comparison study of alkali metal-doped g-C₃N₄ for visible-light photocatalytic hydrogen evolution, *Chin. J. Catal.*, 38 (2017) 1981-1989.
- [5] J.-W. Shi, Y. Zou, L. Cheng, D. Ma, D. Sun, S. Mao, L. Sun, C. He, Z. Wang, In-situ phosphating to synthesize Ni₂P decorated NiO/g-C₃N₄ p-n junction for enhanced photocatalytic hydrogen production, *Chem. Eng. J.*, 378 (2019) 122161.

[6] X. Li, H. Zhang, Y. Liu, X. Duan, X. Xu, S. Liu, H. Sun, S. Wang, Synergy of NiO quantum dots and temperature on enhanced photocatalytic and thermophoto hydrogen evolution, *Chem. Eng. J.*, 390 (2020) 124634.